Journal of Imaging Science and Technology® 54(1): 010504–010504-6, 2010.

Probing Interfacial Acid-Base Interactions in Ink-Substrate Adhesion

Manoj K. Bhattacharyya▲, **Hou T. Ng**▲ **and Eric G. Hanson**▲
HP Laboratories, Hewlett-Packard Company, 1501 Page Mill Road, Palo Alto, California 94304
E-mail: hou-t.ng@hp.com

Bruce J. Jackson and Stanley D. Morse
HP Indigo R&D Division, Hewlett-Packard Company, 11311 Chinden Blvd., Boise, Idaho 83714

Marc Aronhime
Hewlett-Packard Indigo Ltd. (Israel), Einstein 10, Kiryat Weizmann, Ness Ziona, Rehovot 76101, Israel

Abstract. *Ink-substrate adhesion critically impacts the print and page attributes of advanced printing technologies. Here the authors show that interfacial acid-base interaction (A-BI) plays an important role in the enhancement of ink-substrate adhesion. Successful probing of the ink-substrate interface via surface-sensitive attenuated-total-reflectance Fourier-transform infrared spectroscopy reveals intricate transient A-BI behavior, which appears to dominate the initial phase of adhesion in a printed substrate. The authors also demonstrate that macroscopic adhesion strength between an ink layer and a substrate can be correlated directly to the extent of A-BI. Their observation could potentially pave new directions for future advancement of high speed digital printing technology and could have important implications in other marking material systems.* © *2010 Society for Imaging Science and Technology.*
[DOI: 10.2352/J.ImagingSci.Technol.2010.54.1.010504]

INTRODUCTION

Adhesion of materials to a substrate plays an important role in many processes, ranging from biological systems[1] to industrial applications.[2] Very often, tweaking of the interfacial physicochemical interactions affects the desired outcome of a process.[3]

In the arena of advanced digital printing technology,[4] an excellent interfacial adhesion between a marking material, typically an ink particle, and a substrate, generally a paper or a plastic, can provide important print and page attributes—visually pleasant image quality, typically represented by high print durability for rub resistance, water and smear fastness, and overall throughput of a printing process. With the advent of high speed digital commercial printing based either on the liquid[5] or dry electrophotographic printing processes,[6] this becomes critical.

Significant efforts have occurred to facilitate good adhesion of ink particles on a wide range of substrates. For example, thermal-induced fusing via mechanical interlocking of ink particles onto a substrate is known to facilitate reasonably good adhesion.[5] Besides, tailoring of interfacial electrostatic and van der Waals interactions have been demonstrated to enhance ink adhesion to substrates.[7] In addition, coating of a polymer, which acts as a primer on a substrate to facilitate hydrogen bondings (HBs) and/or acid-base interactions (A-BIs), has been shown to noticeably improve ink-substrate adhesion and hence the so-called paper gamut.[8,9]

In particular, the HBs and or A-BIs are thought to play critical roles in the liquid electrophotographic (LEP) printing process (Figure 1) and are clearly iterated by the total reversible work of adhesion W_A as $W_A=(W_{ab}+W_d)$,[10] where W_A is defined as the energy required to break a unit area of an adhesional contact. In this case, it is a measure of the "fundamental" adhesion between an ink layer and a substrate. Here, W_{ab} denotes the acid-base interaction component, while W_d denotes the dispersion component. The later typically involves Lifshitz–van der Waals interaction, which produces a certain "basic level" of adhesion. However, in practice, it is not highly dependent on the nature of the interacting materials.[11]

For most polymer-fiber systems, W_d's are comparable and have been shown to not being able to account for the

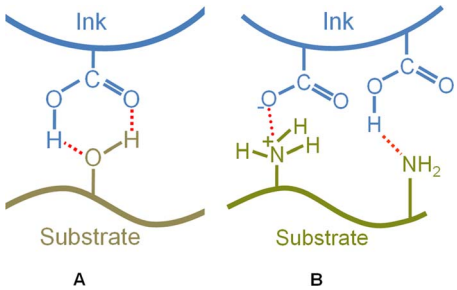

Figure 1. A schematic illustrating hydrogen bonding interaction between a carboxylic group and a hydroxyl group (A) and acid-base and hydrogen bonding between an amine and carboxylic group (B). Hydrogen bonding and acid-base are commonly termed as acid-base interaction. Red dotted lines denote the acid-base interaction between two chemical functional groups.

▲IS&T Member.

Received Jun. 19, 2009; accepted for publication Jul. 31, 2009; published online Dec. 23, 2009.
1062-3701/2010/54(1)/010504/6/$20.00.

Table I. Atomic percent ratio of elemental carbon, oxygen, and nitrogen among the four papers.

	Total C (at. %)	Total O (at. %)	Total N (at. %)	(O+N)/C (%)
P1 (UC)	61.5	35.5	0.9	59.2
P2 (UC)	66	23.5	8.5	48.5
P3 (C)	53.5	33.2	0.0	62.1
P4 (C)	45.6	40.1	0.3	88.6

considerable adhesion strength (i.e., "practical" adhesion) differences observed. On the other hand, promoting W_{ab} by increasing the electron-donor capability at the interfaces generally results in an increase of both the fundamental and practical adhesion.[11] However, its distinctive transient role in such an interfacial interaction is poorly understood, particularly, for polymeric ink-paper interactions. Since ink-paper interactions in LEP are essentially a surface phenomenon and occur across a narrow interfacial boundary, probing of the interfacial interactions pose a significant challenge. Although surface-sensitive techniques, such as attenuated-total-reflectance Fourier-transform infrared spectroscopy (ATR-FTIR) and x-ray photoelectron spectroscopy have been reported to successfully investigate various interfaces,[12–16] probing of ink-paper interfaces remains a significant challenge. Two major showstoppers are the interferences coming from the nonuniformity of the ink layer and the uneven surface topography of the printed papers, especially for cellulose-based papers.

We show here that intricate transient behavior pertaining to interfacial A-BI of ink particles and papers can be readily revealed via the ATR-FTIR spectroscopic technique, upon careful control of the ink thicknesses on the paper. Correlations with adhesion strength of an ink layer on various substrates, more specifically, cellulose-based papers, agree well with the enhancement of A-BIs.

To mimic the acid-base interactions between an ink particle and a paper, as depicted in Fig. 1, we have adopted an ink particle, which is a controlled blend of polymers like methacrylic acid (MAA) and acrylic acid (AA) copolymers with polyethylene and several other additives.[17] The copolymers provided the desired carboxylic groups (−COOHs), while the hydroxyl groups (C−OHs) and the amine groups (−NH, −NH2, or −NH3) were derived from four representative papers, designated P1–P4, featuring varying concentrations of the latter two (Table I). Common sources of C−OHs include polyvinyl alcohol, polyethylene glycol, starch, and carboxymethyl cellulose. A common source of amine in the paper industry is polyethyleneimine, which is often found to consist of a mixture of primary, secondary, and tertiary amines. These are typically used as the binders or cobinders, to be added to the coating pigments, in the paper manufacturing process.[8] When a spatially accessible −COOH on the ink particle's surface comes in close proximity to a surface −OH or −NH of a paper, either hydrogen bonding or acid-base reaction may be anticipated to occur.

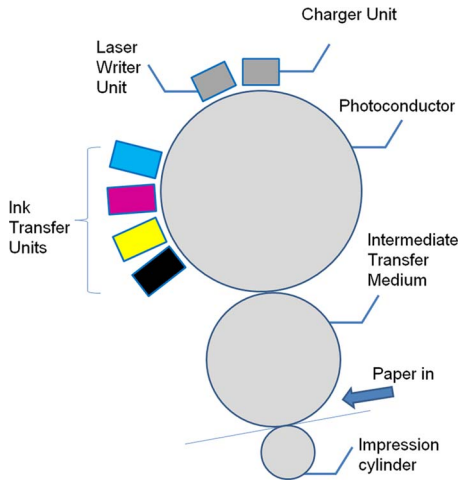

Figure 2. Schematic of an LEP printing press used in this study.

METHODS AND MATERIAL

Liquid Electrophotographic Printing

LEP is a variation from the conventional dry electrophotography (DEP).[5] LEP uses a liquid toner for printing instead of the conventional dry toner particles typically used in DEP. As depicted in Figure 2, in a regular printing process, a photoconductor is first charged uniformly by a charging unit; charging is then followed by exposure to a laser beam (e.g., via a laser scanner) to create a latent image on the photoconductor. A liquid toner, which contains ink particles suspended in an isoparaffinic oil, is subsequently developed onto the photoconductor in a controlled fashion to form a uniform ink layer. The ink layer thickness on the photoconductor can be controlled by changing the electric fields in the developer units. The ink layer is then transferred to a so-called intermediate transfer medium, which is maintained at an elevated temperature (~90°C) before printing onto a piece of paper.

In the present work, we used an HP (Hewlett-Packard)-Indigo 5500 digital press (Hewlett-Packard Co., Palo Alto, CA) to print ink layers with various thicknesses on P1, P2, P3, and P4 from ~0.5 to 6 μm.

Sample Configurations and X-Ray Photoelectron Spectroscopy

Table I lists four commercially available papers used in the present study. P1 and P2 are uncoated (UC) papers while P3 and P4 are coated (C) papers. One of the major differences between P1 and P2 is a surface treatment with polyethyleneimine on P2. In general, all of these papers exhibit acceptable or enhanced levels of practical adhesion for LEP printing.

Surface elemental compositions were obtained via x-ray photoelectron spectroscopy (XPS) using the PHI Quantum 2000 system. A monochromated Al $K\alpha$ 1486.6 eV x-ray source was used for probing the surfaces. An analysis area of ~1300 by 300 μm was used for the XPS measurements. All XPS data were quantified based on respective relative sensitivity factors. The relative percentage of the total polar com-

ponents' concentration on the paper top surface is also provided, as this ratio is sometimes taken as an indication of the polar reactivity between ink and paper.

ATR-FTIR

ATR-FTIR spectroscopy was used to characterize the ink-paper interface as well as the surfaces of papers and ink particles. All measurements were done on a Nicolet Nexus 870 spectrometer equipped with a liquid nitrogen cooled mercury cadmium telluride detector. A single reflection Harrick Scientific germanium IRE with an incident angle of 65° was used. Nitrogen was used as the purging gas. A resolution of 1 cm^{-1} with a total of 64 scans was used for all the measurements.

Adhesion Strength Measurement

We have adopted a method similar to that reported by Zhao et al.[18] First, a half-inch pressure-sensitive tape (3M Co., St. Paul, MN, No. 401B) was pressed onto an ink layer and then pulled with a specified transversal speed using a ChemInstruments AR1000 adhesion tester at an angle of 180°. When measurable detachment of ink particles was detected visually, the pulling force and the traversal speed (TS) of the pulling tape were recorded. For measurable ink particle detachment, we have assumed a 10% ink layer surface damage (i.e., the ink detachment may not occur completely) as the threshold. A graph of the work per unit area of the tape versus the pulling speed was then plotted. To compensate for the input energy needed to deform the tape and the paper, the effective adhesion strength is determined from the intercept of the y-axis at TS$=0$ ms^{-1}. The use of a linear scale for TS was seen effective as compared to the logarithmic approach reported by Zhao et al.[18] High repeatability was routinely obtained using a similar set of measuring and preparing tools.

RESULTS AND DISCUSSION

Importance of Ink Layer Thickness Control

To probe the intricate interfacial interactions between an ink layer and a paper surface via the surface-sensitive ATR-FTIR spectroscopy, we have used an LEP printing process to controllably obtain continuous thin films of ink particles with desired thicknesses of ~0.5 and ~5 μm. The importance of ink layer thickness control can be understood by considering the penetration depth of the evanescent wave in an ATR-FTIR measurement.[16] A thin, smooth, and continuous ink layer is needed for successful and unambiguous probing of the ink-paper interface layer by the evanescent wave. Through a trial and error process of optimizing the printing process and a judicious guess of the refractive index of the black ink used in the present study, we infer that an appropriate ink thickness of around 0.5 μm is highly to be desired. With an ink layer thickness higher than this critical thickness, one measures solely the bulk ink characteristics (bulk ink is denoted as thick ink in the subsequent discussion) and does not probe the ink-paper interface, whereas a thinner ink layer imposes practical implementation difficulty due to discontinuity of the printed layer.

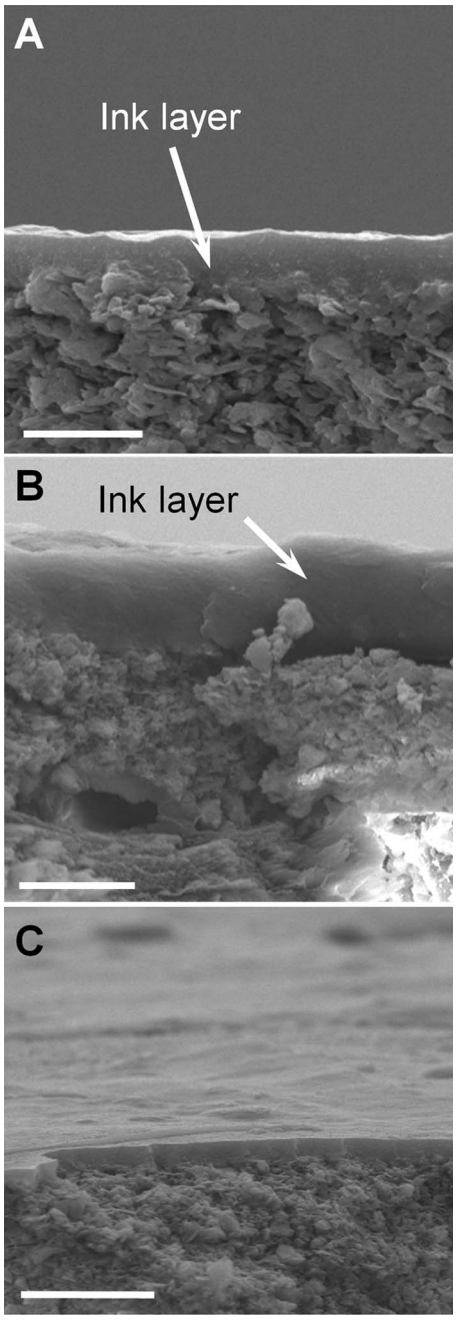

Figure 3. Scanning electron microscopy (SEM) of ink layers on a paper. (A) A cross-sectional SEM image of a thin ink layer on a coated cellulose-based paper. The thickness of the ink layer is ~0.55 μm. Note the smoothness of the ink layer surface topography. Scale bar: 2 μm. (B) A cross-sectional SEM image of a relatively thick ink layer on a paper similar to (A). The film thickness was obtained by printing multiple times with a HP-Indigo 5500 digital press. Scale bar: 5 μm. (C) A perspective view of the thin ink layer on a paper. Note again the smoothness of the surface topography. Scale bar: 5 μm.

Figures 3(A) and 3(B) show cross-sectional SEM images of both ink layers on a paper. As shown in Fig. 3(C), we noticed complete coverage of the underlying substrate with an ink layer of 0.5 μm. We also noted the relative smoothness of both ink layers, which is conducive toward investigating the interfacial physicochemical interactions via ATR-FTIR spectroscopy by facilitating enhanced optical contact while suppressing undesirable signal scatterings.

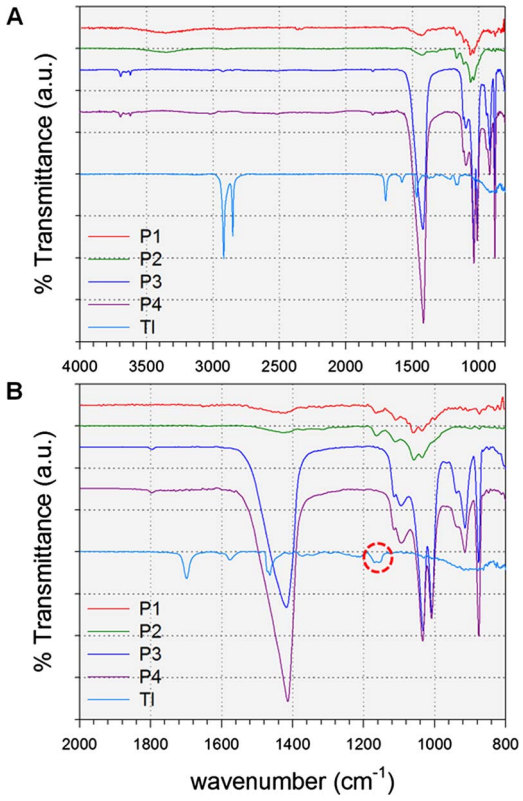

Figure 4. ATR-FTIR spectra of the four papers and a thick ink layer. The dashed circle in Fig. 4(B) indicates the region of interest, which reveals the acid-base interactions.

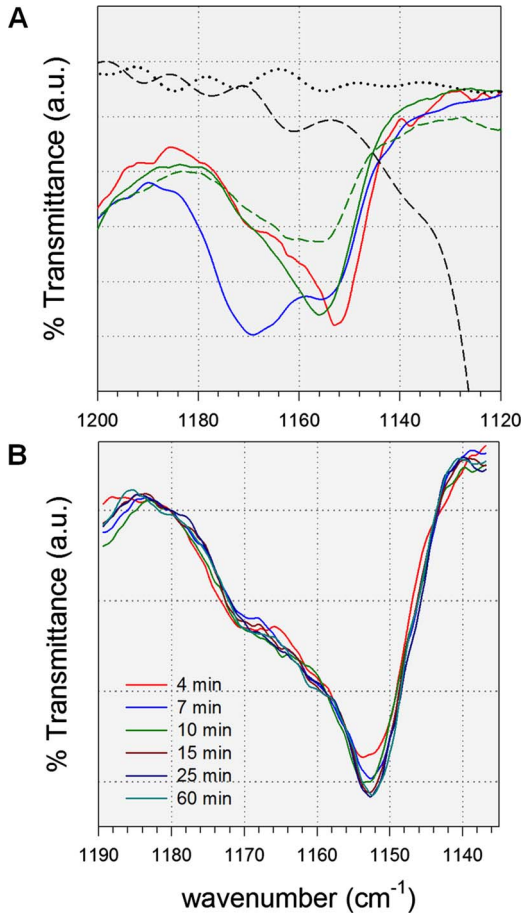

Figure 5. ATR-FTIR spectroscopic investigation of interfacial A-BIs. (A) ATR-FTIR spectra revealing the differences among the individual components of an ink particle, coated paper P4, thin and thick ink layers in the region of interest—between 1120 and 1200 cm^{-1}. Red: thin ink layer; blue: thick ink layer; solid green: acrylic acid copolymer; dotted green: methacrylic acid copolymer; and dash black: P4 and dotted black: polyethylene. (B) ATR-FTIR mapping of the transient A-BI behavior at regular intervals after printing a thin ink layer on P4. All spectra were baseline-corrected and overlaid accordingly.

ATR-FTIR Measurement of Four Papers, Thick Ink, and Thin Ink

Figure 4 shows the ATR-FTIR spectra of the four paper samples, as shown in Table I, and also that of a thick ink, as shown in Fig. 3(B). Major signature peaks are seen from either the paper coating or the filler materials: $CaCO_3$ at 1444 (broad), 1796, 874, and 713 cm^{-1}, Kaolin clay at 1007, 1036, 1111, and 913, and twin bands at 3696 and 3621 cm^{-1}.[19] The thick ink (~4 μm in this measurement) shows a characteristic carbonyl (C=O) peak at 1700 cm^{-1} and −CH2 stretching bands at 2920 and 2850 cm^{-1}. Of particular importance is a narrow region marked with a dashed circle, as shown in Fig. 4(B) and further explored in Figure 5.

The importance of controlling ink layer thickness in order to reveal a key signature peak which is indicative of A-BI is clearly seen in Fig. 5(A). We observe two distinctive bands for both ink layers, one commonly centered at ~1169 cm^{-1} and the other at ~1156 and 1152 cm^{-1}, respectively, for the thick and thin ink layers. To elucidate the origins of these vibrations, we have acquired individual FTIR spectra of the ink particle's components, namely, polyethylene, MA, and AA copolymers. It is obvious that these two bands have no direct associations with polyethylene and the paper P4, which has the highest polar component concentration among the four papers employed in this study. By Gaussian—Lorentzian curve fitting of these profiles after respective baseline corrections, we assign the bands centered at ~1169 cm^{-1} to the C−C stretching vibrations and the bands at ~1156 cm^{-1} to the O−C−O bond of the carboxylic group.[20]

Unlike the case of the thick ink layer, a downshift of ~4 cm^{-1} to ~1152 cm^{-1} is noted for the thin ink layer. In addition, we observe a relative increase in intensity of C−O stretching vibration (sv), as compared to the nearby C−C sv. With assignment of the C−O sv intensity as IR_2 and that of the C−C sv as IR_1, the ratio IR_2/IR_1 increases from 0.9 (for the thick ink) to 2.5 (for the thin ink). Taking into consideration the penetration depth of the IR evanescent wave, we strongly believe that we have successfully probed the ink-substrate interface and that the downshift is likely due to acid-base interaction of the −COOH with −OH of the underlying paper. It is important to note that similar trends were observed for the other three papers [Figures 6(A)–6(C)] even though their −OH or −NH concentrations are lower than that of P4. Further evidence of such an A-BI is provided by the suppression of the dimeric −COOH band intensity at around 3100 cm^{-1} and the slight

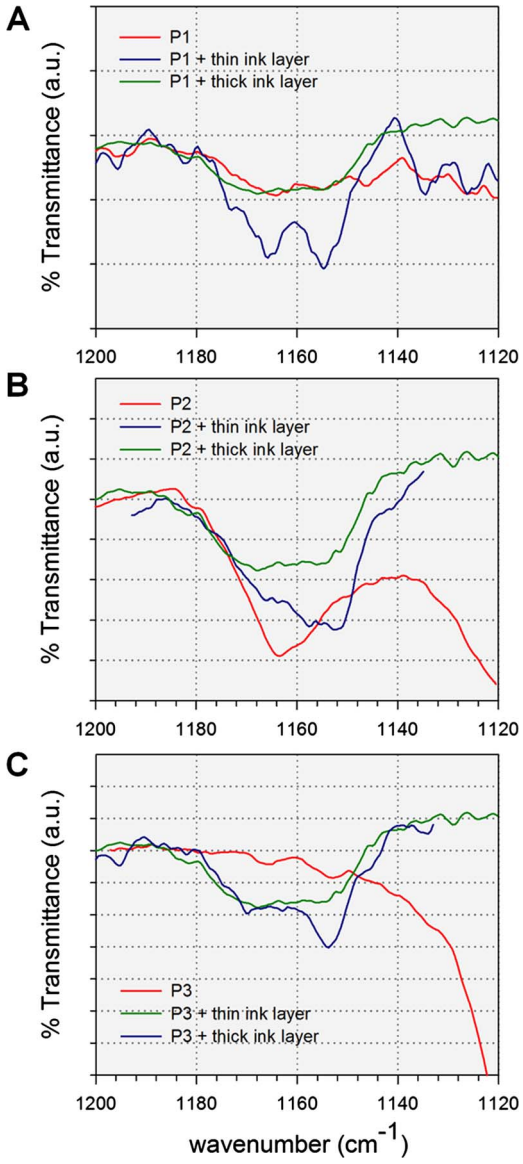

Figure 6. ATR-FTIR spectra of respective blank paper, thick ink, and thin ink for P1, P2, and P3.

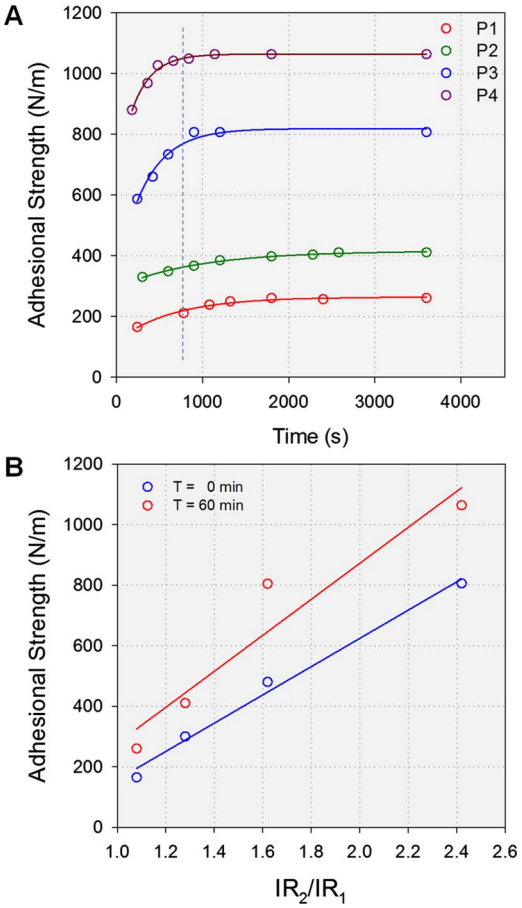

Figure 7. Adhesion strength evolution and its correlation with the extent of A-BIs. (A) Adhesion strength vs time evolution for P1, P2, P3, and P4. (B) Correlation of A-BIs to ink-substrate adhesion strength at $t=0$ s and $t=3600$ s.

appearance of monomeric −COOH at ~3500 cm^{-1}.[19] Although it has been reported in some cases that a dehydration reaction between −OH and −COOH could occur,[21] we failed to observe such a reaction in this work. This is likely due to the relatively short duration (~150 μs) of the nip contact, i.e., during the transfer of the heated ink particles from the intermediate transfer medium to the paper at ~90°C. Further supporting evidence is given by the band centered at 1700 cm^{-1}, which coincides with those of MAA, AA, and the thick ink layer, and suggests the presence of carbonyl group of −COOH.

Temporal Evolution of Acid-Base Interaction

Next, we studied the temporal evolution of the transient A-BI between a thin ink layer and a paper surface. Immediately upon printing the ink layer onto P4, we tracked changes of the signature peaks at both 1169 and 1152 cm^{-1}. As shown evidently by the band position at ~1152 cm^{-1} in Fig. 5(B), within the first 4 min after printing, more than 80% of the A-BI has taken place, as compared to that of Fig. 5(A), which was acquired after 1 h of printing. Interestingly, we observe that ~15 min after printing, near complete A-BI has occurred. On the other hand, no noticeable changes were seen for the bands centered at 1169 cm^{-1}.

Macroscopic Adhesion Strength and Acid-Base Interaction

More importantly, we have consistently observed that the transient A-BI behavior manifested itself through macroscopic measurement of the adhesion strength or the "practical" adhesion. It should be pointed out that typical experimentally measured adhesion strength values reflect the interfacial adhesion indirectly and may be influenced not solely by physicochemical interfacial interactions but also mechanical properties of the paper matrix.[11] To simplify the present study, we have selectively chosen papers which possess excellent structural mechanical property and do not show fiber failure during our adhesion tests.

Figure 7(A) profiles the adhesion strength evolutions for the four representative papers. We observe that for each profile, the adhesion strength increases exponentially to a near-flat plateau in less than 20 min. Based on the relative strength and kinetics of acid-base and van der Waals

interactions,[22,23] and the transient A-BI behavior as shown in Fig. 5(B), we suggest that at time $t=0$ s or soon thereafter (measured at regular intervals after printing), A-BI dominates the ink-substrate interaction. However, the contribution of van der Waals interaction to the adhesion strength should not be completely ruled out. During the transfer of ink particles onto the paper surface, a minute amount of the isoparaffinic oil (i.e., liquid carrier of the ink solution) is likely to be carried over and trapped in between the ink-paper interface. As the liquid carrier wicks away from the interface, a van der Waals interaction is expected to take effect.

Hence, it is reasonable to divide the profiles into two working regimes. In regime 1, the adhesion strength increases rapidly and is governed mainly by A-BI. In regime 2, van der Waals interaction dominates the practical adhesion. A transition should exist between regimes 1 and 2, where the incremental dispersion component becomes higher than the incremental A-BI component.

The exact duration of this transition is expected to be a strong function of the paper surface porosity and surface roughness. It is thus logical to assume that if the adhesion strength versus time profiles are extrapolated to $t=0$ s, the A-BI component of W_A could be obtained, as shown in Fig. 7(B) (i.e., the blue-colored profile). The almost perfect linear fit is striking and reinforces the supposition that short time adhesion is dominated by the A-BI between ink and paper. Figure 7(B) shows the final adhesion strength obtained with these four papers versus the A-BI component (the blue-colored profile). The difference between the red and blue profiles represents the van der Waals component of the adhesion strength.

CONCLUSION

In conclusion, we show the important role of A-BI toward enhancing ink-paper adhesion strength. The LEP printing process has been demonstrated to be an ideal approach for laying down high-quality continuous smooth thin films of ink particles and could serve as an appropriate testbed for the investigation of advanced material sets for future high speed digital printing.

ACKNOWLEDGMENTS

The authors gratefully acknowledge the many valuable discussions with their colleagues Tom Anthony, Kris Nauka, Michael Lee, Gana Ganapathiappan, Paul McCaslin, Gary Larson, Omer Gila, Elliad Silcoff, and Albert Teishev.

REFERENCES

[1] H. F. Lodish, *Molecular Cell Biology* (W. H. Freeman and Co., New York, 2008).
[2] *Handbook of Adhesion*, edited by D. E. Packham (Wiley-Interscience, New York, 2005).
[3] D. M. Brewis and D. Briggs, *Industrial Adhesion Problems* (Wiley-Interscience, New York, 1985).
[4] P. K. Bennett, H. R. Levenson, and F. J. Romano, *The Handbook for Digital Printing and Variable-Data Printing* (Graphic Arts Technical Foundation, Pittsburgh, PA, 2006).
[5] G. Tzori, *Proc. IS&T's NIP20: International Conference on Digital Printing Technologies* (IS&T, Springfield, VA, 2004), p. 586.
[6] http://www.reuters.com/article/pressRelease/idUS160604+25-Feb-2008+MW20080225.
[7] D. S. Rimai, D. S. Weiss, and D. J. Quesnel, J. Adhes. Sci. Technol. **17**, 917 (2003).
[8] *Handbook of Paper and Board*, edited by H. Holik (Wiley-Interscience, New York, 2006).
[9] S. L. Webb, M. Aronhime, and P. Forgacs, *Research Disclosure* (U.S. Patent Office, 2006), Vol. 511, p. 1463..
[10] W. Gutowski, R. J. Good, M. K. Chaudhury, and C. J. van Oss, in *Fundamentals of Adhesion*, edited by L.-H. Lee (Plenum, New York, 1991), pp. 87–172.
[11] E. Pisanova and E. Mäder, J. Adhes. Sci. Technol. **14**, 415 (2000).
[12] T. Lummerstorfer and H. Hoffmann, Langmuir **20**, 6542 (2004).
[13] T. Lummerstorfer, C. Sohar, G. Friedbacher, and H. Hoffmann, Langmuir **22**, 18 (2006).
[14] K. Fa, T. Jiang, J. Nalaskowski, and J. D. Miller, Langmuir **20**, 5311 (2004).
[15] M. R. Yalamanchili, A. A. Atia, and J. D. Miller, Langmuir **12**, 4176 (1996).
[16] K. Vikman and K. Sipi, J. Imaging Sci. Technol. **47**, 139 (2003).
[17] P. Ben-Avraham, B. Bossidan, and B. Landa, US Patent No. 7,078,141, B2 (2006).
[18] B. Zhao, L. Anderson, A. Banks, and R. Pelton, J. Adhes. Sci. Technol. **18**, 1625 (2004).
[19] G. Socrates, *Infrared and Raman Characteristic Group Frequencies* (John Wiley and Sons Ltd., West Sussex, England, 2006).
[20] T. Kobayashi, H. Y. Wang, and N. Fujii, Anal. Chim. Acta **365**, 81 (1998).
[21] M. Fichet, G. Dutier, A. Yarovitsky, P. Todorov, I. Hamadi, I. Maurin, S. Saltiel, D. Sarkisyan, M.-P. Gorza, D. Bloch, and M. Ducloy, Europhys. Lett. **77**, 54001 (2007).
[22] L. C. Allen, Proc. Natl. Acad. Sci. U.S.A. **72**, 4701 (1975).
[23] In-house measurement of pure samples.